LUMINESCENCE DATING OF YOUNG COASTAL DEPOSITS FROM NEW ZEALAND USING FELDSPAR

ANNI T. MADSEN[1], JAN-PIETER BUYLAERT[2,3] and ANDREW S. MURRAY[2]

[1]*Department of Geography and Geology, University of Copenhagen*
Øster Voldgade 10, DK-1350 Copenhagen K, Denmark
[2]*Nordic Laboratory for Luminescence Dating, Department of Earth Sciences, Aarhus University,*
Risø National Laboratory for Sustainable Energy, Denmark
[3]*Radiation Research Division, Risø National Laboratory for Sustainable Energy,*
Technical University of Denmark (DTU), Denmark

Abstract: A new measurement protocol has been tested on K-feldspars from Whanganui Inlet and Parengarenga Harbour, New Zealand. A Single Aliquot Regenerative (SAR) dose protocol, using two successive infrared (IR) stimulations (post-IR IR SAR protocol) is setup for these young (<1000 years) coastal sediments. Significant anomalous fading (g_{2days}=7 %/decade) is observed using the conventional IR signal measured at 50°C. In contrast, the fading rate of the IR signal measured at elevated temperature (150°C) after the IR stimulation at 50°C (a post-IR IR signal) is not significant ($g_{2days} \leq 1$ %/decade). Surprisingly low residual infrared stimulated luminescence (IRSL) signals were observed for a surface sample, suggesting that accurate ages as young as ~50 years can be obtained for these recent deposits. IRSL ages ranging between 48±6 years and 1050±50 years are obtained from six samples, indicating that sediment accumulation has occurred at the two sites during the last millennia, despite a falling trend in relative sea-level in Whanganui Inlet and a stable relative sea-level at Parengarenga Harbour.

Keywords: Luminescence dating, IRSL, K-feldspar, young sediments, New Zealand.

1. INTRODUCTION

Over the last few years luminescence dating has been more and more widely applied in studies of marine deposits and coastal change, and a large body of literature has become available describing the use of this dating technique on many types of coastal deposits, addressing a diverse range of local, regional and global issues. A comprehensive review by Jacobs (2008) compiles all these coastal studies and a review by Madsen and Murray (2009) summarizes the dating of young (<1000 years) coastal and aeolian sediments. So far, a limited number of

studies have been published from coastal sites in New Zealand (Duller, 1996; Shulmeister *et al*. 1999; Rees-Jones *et al*. 2000; Nichol, 2002; Litchfield and Lian, 2004; Cooper and Kostro, 2006; Kennedy *et al*. 2007) and these have focused mainly on Pleistocene deposits (older than 10,000 years). Only Shulmeister and Kirk (1996) and Nichol *et al*. (2003) present chronologies on a millennial time-scale of Holocene (younger than 10,000 years) dune ridges. There has been almost no work on recent deposition of relevance to coastal management and pollution studies.

In some locations quartz has limited applicability because of low luminescence sensitivity (light output per unit dose). For instance, Preusser *et al*. (2006) concluded that the quartz from glacial sediments from the New

Zealand Alps (Westland, South Island) was an unsuitable dosimeter for luminescence dating because of apparent low luminescence intensity and large sensitivity changes during the multiple measurement cycles in the Single Aliquot Regenerative (SAR) dose protocol. It is not known whether this problem prevents the use of quartz in the dating of very young/recent coastal New Zealand sediments.

Potassium-rich feldspar is an alternative dosimeter; it has the advantage that it is more likely to be sensitive, and so provides a measurable signal, but there are also disadvantages associated with this mineral. The solar resetting process occurs much more slowly for feldspar than for quartz (e.g. Godfrey-Smith *et al.* 1988). If the measurement of burial dose is to be accurate, then it is clearly very important that any trapped charge is completely reset prior to burial; the smaller the dose to be measured (as in very young sediments) the more important it is that this resetting process is complete (Madsen and Murray, 2009). Moreover, K-feldspar suffers from anomalous fading (Wintle, 1973); this expresses itself as an unexpected loss of luminescence signal with time, despite kinetic studies indicating that the signal should remain stable (Aitken, 1985). Reports of luminescence chronologies from New Zealand have shown that investigations based on either quartz or feldspar may run into difficulties (Duller, 1994a, 1994b; Pillans *et al.* 1996; Berger, *et al.* 2001; Almond *et al.* 2001, 2007; Preusser *et al.* 2006) due to anomalous fading in the case of feldspar and low luminescence sensitivity in the case of quartz.

This study aims to test the suitability of luminescence dating for establishing chronologies on a decadal to centurial time-scale on coastal New Zealand sediments. The use of both quartz and feldspar is explored. Most luminescence studies based on feldspar have employed infrared (IR) stimulation at 50°C (here abbreviated IR@50°C) and detection in the blue spectrum (e.g. Auclair *et al.* 2007; Wallinga *et al.* 2007; Buylaert *et al.* 2011; Davids *et al.* 2010). However Thomsen *et al.* (2008) concluded that the fading rate of these conventional IR signals is significantly higher than the fading rate of IR signals measured at an elevated stimulation temperature (e.g. 150°C) after an IR@50°C (here called post-IR IR@150°C). Buylaert *et al.* (2009) confirmed that this is also true in nature. In this study, we first test the sensitivity of quartz from 17 sites around the New Zealand coastline, and then test the application of a new post-IR IR Single Aliquot Regenerative (SAR) dose protocol on K-rich feldspars from two sites. The ability of our protocol to recover a known dose given in the laboratory before heating is examined, and the laboratory fading rates are measured for both the IR@50°C and post-IR IR@150°C. The degree of bleaching is also examined using the most recently deposited material and the resulting post-IR IR ages.

2. STUDY AREAS

Preliminary investigations of the luminescence properties of quartz were undertaken on modern material taken from beach deposits at 17 different coastal locations in New Zealand (see **Table 1** and **Fig. 1**). In addition, more detailed studies using K-feldspar were undertaken at one of these sites (Parengarenga) and at an additional site (Whanganui). The latter two sites are described in more detail below:

Parengarenga Habour

Parengarenga Harbour is a ~63 km^2 large meso-tidal estuary (tidal range ~2 m; Hayes, 1979) with generally less than ten metres water depth. The average volume of water exchanged during a tidal cycle is 25×10^6 m^3 (Heath, 1975) and fresh water input amounts to ~7 m$^3 \cdot$s^{-1} on average (Heath, 1976). The lagoon is located at the northernmost part of the Aupouri Peninsula in the far north of North Island (**Fig. 1**). The Northland area is generally accepted to be tectonically stable (Litchfield, pers. comm. 2010) and relative sea-level is thought to have been stable within ±0.2 m during the last ~6500 years (Wellman, 1962; Gibb, 1986). Fluvial sediment input into Parengarenga Harbour is small; the largest fraction of the total sediment input is marine-derived (Pritchard *et al.* 1998). Inter-tidal sediments in Parengarenga Harbour are dominated by fine quartz-rich sands (silica content >95%); inter-tidal mud is restricted to the very upper reaches of the estuary. The sand within the harbour is part of the Parengarenga Sand Facies defined by Schofield (1970). Three 5 cm thick inter-tidal samples (095502, 095503 and 095504) were taken from a shallow sediment core retrieved from Parengarenga Harbour (sample 095502 includes the modern surface). Sampling was not far from one of the relatively large tidal channels so the sediment may reflect point-bar sedimentation from migration of this channel rather than simple tidal flat deposition. A further sample (095501) was taken from an aeolian dune known to have formed since 1982; the evolution of the fore-dune has been surveyed in detail by sequential levelling (Parnell *et al.* 2003; pers. comm.).

Whanganui Inlet

Whanganui Inlet is a narrow estuary, 13 km long and up to 3 km wide (~40 km^2), located in the north-western part of South Island (**Fig. 1**). It has a semi-diurnal tide with a mean range of 3 m (Davidson, 1990) defining it as a meso-tidal estuary (Hayes, 1979). The average tidal prism is 20×10^6 m^3 (Heath, 1975). Numerous small streams drain into the lagoon, resulting in an average freshwater input of ~4 m$^3 \cdot$s^{-1} from the 216 km^2 catchment (Heath, 1976). The dominant sediment source is thought to be these small streams (Armour and Kennedy, 2005). Relative sea-level has been decreasing slowly, due to local tectonic uplift during the Holocene (Litchfield, pers.
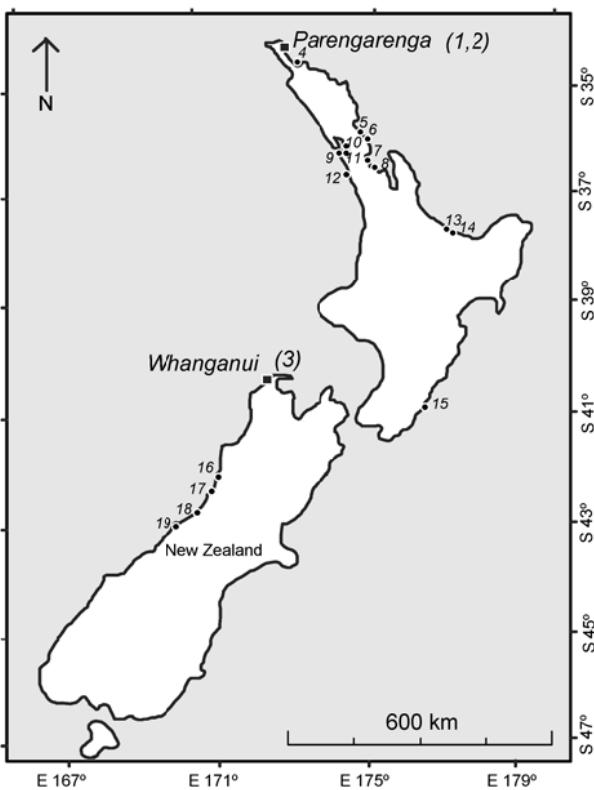
Fig. 1. *Map displaying the nineteen sample locations in New Zealand; the main sites Parengarenga Harbour and Whanganui Inlet are highlighted.*

Table 1. *GPS coordinates of sample locations. NI: North Island, SI: South Island.*

Sites	No		Coordinates
Parengarenga	1	Northland, NI (aeolian)	S 34°32' 19.77" E 172°59' 23.12"
Parengarenga	2	Northland, NI (inter-tidal)	S 34°31' 42.12" E 172°58' 52.49"
Whanganui*	3	Northeast coast, SI (salt-marsh)	S 40°35' 58.51" E 172°34' 50.56"
Eastern beach	4	Northland, NI	S 34°53' 05.57" E 173°16' 13.21"
Mangawhai	5	east coast, north of Auckland, NI	S 36°05' 32.88" E 174°36' 05.64"
Omaha Beach	6	east coast, north of Auckland, NI	S 36°19' 10.62" E 174°46' 45.75"
Orewa Beach	7	east coast, north of Auckland, NI	S 36°35' 52.15" E 174°42' 03.71"
Long Bay Beach	8	east coast, north of Auckland, NI	S 36°41' 48.17" E 174°44' 54.53"
Kaipara Harbour	9	west coach, north of Auckland, NI	S 36°23' 13.27" E 174°44' 54.53"
Tapora	10	west coach, north of Auckland, NI	S 36°22' 57.26" E 174°18' 12.07"
Tauhoa	11	west coach, north of Auckland, NI	S 36°25' 34.40" E 174°26' 27.16"
Piha Beach	12	west coast, north of Auckland, NI	S 36°57' 25.95" E 174°28' 03.57"
Ohiwa Beach	13	Bay of Plenty, NI	S 37°59' 18.40" E 177°09' 18.96"
Waiatahi estuary	14	Bay of Plenty, NI	S 37°59' 29.97" E 177°11' 57.46"
Castle Point Inlet	15	Southeast coast, NI	S 40°54' 16.60" E 176°13' 41.42"
Taramakau	16	west coast, SI	S 42°33' 02.17" E 171°08' 12.36"
Hokitika	17	west coast, SI	S 42°43' 17.55" E 171°57' 12.37"
Okarito Lagoon	18	west coast, SI	S 43°13' 12.00" E 170°11' 13.98"
Gillespies	19	west coast, SI	S 43°13' 21.80" E 169°49' 15.92"

note that Q was not investigated at this site

comm. 2010). Whanganui inlet forms a structurally-controlled estuary with most of the area made up of mud-flats and sand flats exposed at low tide (Kennedy *et al.* 2008). The present surface morphology of Whanganui Inlet appears to be inherited from sedimentation that took place soon after the sea-level drop slowed up and stabilised; contemporary sedimentation on these tidal flats is therefore thought to be small (Kennedy *et al.* 2008). Armour and Kennedy (2005) argued that the tidal flats in Whanganui Inlet accreted rapidly after the postglacial marine flooding, based on radiocarbon ages of ~7 ka at a depth of only 1.8 m, and so the tidal flats are thought to have reached modern elevations soon after initial sea-level flooding (Kennedy *et al.* 2008). Two (2 cm thick) samples (095509 and 095510) were recovered from a salt-marsh deposit fringing the lagoon at respectively 35 cm and 55 cm depth.

3. METHODS

Sample preparation

The 17 modern beach samples used to investigate the luminescence properties of quartz were etched with HCl (10%), H_2O_2 (10%), HF (40%), and finally HCl (10%) once more. In the case of samples taken for feldspar stud-

ies, the cores were opened under subdued orange light and split into two halves; one half for equivalent dose (D_e) measurements (see later) and another half for dose rate estimation (see later). Samples for D_e measurements were first wet-sieved to isolate material in the 106-212 μm and the 80–300 μm grain-size range for Parengarenga and Whanganui, respectively (the larger interval at Whanganui was because of insufficient material). These fractions were then treated with HCl (10%) and H_2O_2 (10%) to remove carbonates and organic material. A K-rich feldspar extract (density <2.58 g·cm^{-3}) was then separated using heavy liquids and etched for 40 min with diluted HF (10%) to remove the outer alpha-irradiated layer from the grains. After etching, any contaminating fluorides were dissolved using HCl (10%).

All luminescence measurements were made with a Risø TL/OSL reader equipped with a ^{90}Sr/^{90}Y beta-source (0.044±0.001 Gy·s^{-1}) and light sources, consisting of blue diodes emitting at 470 nm and IR diodes emitting at 875 nm (Bøtter-Jensen *et al.* 2003). Luminescence was detected in the UV through a U340 glass filter for quartz measurements and in the blue–violet through a Schott BG39/Corning 7-59 glass filter combination for feldspar measurements.

For dose rate determination, samples were dried to laboratory humidity to determine field water content, ignited at 450°C for 24 hours, and subsequently homogenised by grinding to a grain-size of <200 μm. The homogenised samples were mixed with wax, cast in a fixed cup-shaped geometry, and stored for three weeks to allow the establishment of secular equilibrium between ^{222}Rn and ^{226}Ra. Saturated water content was measured on a sub-sample of the unground material.

Preliminary tests on quartz

Large (~8 mm) aliquots of quartz grains were prepared using silicone oil to adhere the grains to a 10 mm diameter stainless steel discs. The purity of the quartz extracts was confirmed by the absence of any IRSL sensitivity. The blue-light stimulated luminescence signals were measured in the usual manner (preheat at 260°C for 10 s and 40 s stimulation at 125°C with 90% blue LED power). These preliminary investigations mostly involved measurement of laboratory test doses (~18 Gy), but the quartz sample from Parengarenga (site number 2) was also used in a dose recovery test, because this sample showed the greatest sensitivity (see section 4).

Equivalent dose measurement on feldspars

For feldspar investigations, small (~2 mm) aliquots containing a few hundred grains were mounted on stainless steel discs with silicone oil. The post-IR IR SAR protocol used in this study (**Table 2**) is based on the protocol proposed by Buylaert *et al.* (2009). For the first

SAR cycle, which measures the natural dose originating from the radiation field present in the natural environment, no laboratory dose was administered. The following SAR cycles measure doses given by a beta source in the laboratory (step 1). The samples were then preheated for 10 s at 180°C (step 2), followed by an IR stimulation at 50°C for 500 s (step 3) and a second IR stimulation for 100 s, when the sample was held at 150°C (step 4); here the luminescence (L_i) is measured. Correction for sensitivity changes throughout the measurement cycles is done by application of a constant test dose (step 5) as part of the SAR procedure (Murray and Wintle, 2000). The test dose (~1.1 Gy) was measured in a similar manner to that used for the natural 'burial' and regenerated doses. The samples are first heated to 160°C (step 6) and then stimulated by IR diodes for 500 s at 50°C (step 7) followed by an IR stimulation for 100 s at 150°C (step 8) where the test dose response (T_i) is measured. After every SAR cycle, the samples are optically bleached using IR diodes for 100 s at 200°C (step 9) to reduce recuperation (Murray and Wintle, 2003). The preheat/cut-heat, stimulation and illumination temperatures are lower than those used by Buylaert *et al.* (2009) because of the expected young age of the sediment and the necessity to reduce thermal transfer as much as possible. In practice, L_i and T_i are calculated using both the IR@50°C and pIRIR@150°C signals, to allowing a comparison of the behaviour of the two signals (L_i and T_i of the IR@50°C signal are measured in steps 3 and 7, respectively). The initial 10 s minus a background derived from the last 50 s was used for calculations with the IR@50°C signal. For the pIRIR@150°C signal the net signal was calculated from the first 1.85 s minus a background from the last 8.9 s.

Fig. 2a shows examples of the natural IR@50°C decay curves from five of the samples and **Fig. 2b** shows the immediately following pIRIR@150°C decay curves. Inset are typical SAR growth curves (corrected IRSL (L_i/T_i) is plotted against laboratory dose; filled circles) for sample 095503. The open circle (recycling point) indicates a repeated measurement and shows that the SAR protocol successfully corrects for sensitivity changes. The recuperation point (triangle at a dose of zero Gy) lies close to, but a little above the origin for the pIRIR@150°C signal. The laboratory dose equivalent to the burial dose is found by interpolation of the corrected natural signals onto the appropriate SAR growth curve and is termed the equivalent dose, D_e (Gy). In all cases, to determine D_e, we assume that the growth curve passes through the origin.

Dose rate

Radionuclide concentrations (in Bq·kg^{-1}) were measured using high-resolution gamma spectrometry (Murray *et al.* 1987). These radionuclide concentrations were then converted to dry infinite matrix dose rates using the conversion factors listed by Olley *et al.* (1996) before the contribution from the cosmic ray dose rate was added

Table 2. *Post-IR IR SAR protocol for K-feldspars (modified after Buylaert* et al. *2009).*

Step	Treatment	Observe
1	Give dose, D_i	
2	Preheat (180°C for 10 s)	
3	Optically stimulate with IR diodes for 500 s @ 50°C	
4	Optically stimulate with IR diodes for 100 s @ 150°C (30 s pause after heating to 150°C)	L_i
5	Give test dose, D_t	
6	Heat to 160°C (< preheat temperature, step 2)	
7	Optically stimulate with IR diodes for 500 s @ 50°C	
8	Optically stimulate with IR diodes for 100 s @ 150°C (30 s pause after heating to 150°C)	T_i
9	Optically bleach with IR diodes for 100 s @ 200°C (> preheat temperature)	
10	Return to 1	

(Prescott and Hutton, 1994). The contribution from internal beta activity from ^{40}K was taken into account based on an assumed effective potassium content of 12.5±0.5% (following Huntley and Baril, 1997). A small contribution to the beta dose rate from ^{87}Rb is calculated assuming a Rb content of 400±100 ppm (Huntley and Hancock, 2001). Estimates of water content were used to reduce the dose rates, using the equations given by Aitken (1985). An average value between the measured field water content and the saturated water content was used in this dose rate correction for the supra-tidal Whanganui samples and the aeolian sample from Parengarenga. The inter-tidal

Parengarenga samples were assumed to always have been saturated because frequent tidal inundations probably maintain the sediment in a near saturated state. The dose rate model by Madsen *et al*. (2005) was applied to take the temporal variability of sample depth into account; this is inevitable when dating young near-surface sediments in accreting environments. The contribution from cosmic ray dose rate decreases as the sediment is buried deeper and deeper but the gamma dose rate increases as the contribution from overlying sediments increases. Radionuclide concentrations (^{226}Ra, ^{232}Th and ^{40}K) are presented in **Table 3**, together with water content and total dose rates.

4. LUMINESCENCE CHARACTERISTICS

Sensitivity of quartz

Fig. 3 shows two representative examples of decay curves from the preliminary quartz tests; the least sensitive (Piha beach, number 12) and the most sensitive (Parengarenga, number 2). In neither case there is a dominant fast component and the material is, in general, very insensitive (only between 800–3000 counts for the first 0.16 s, when a test dose of ~18 Gy is applied; we wish to measure 10–100 mGy natural doses). In addition to low sensitivity, we observed significant sensitivity changes of the quartz from all sites except Parengarenga. A dose recovery test was therefore only undertaken on the quartz from Parengarenga (data not shown). The resulting dose recovery ratios gave a satisfactory mean value of 1.06±0.05 (n=45), but the standard deviation was >30%. This suggests that Parengarenga quartz could probably be used to date old sediment, but not material in the age range of interest here.

Dose recovery test on feldspars

A dose recovery test was undertaken for sample 095502, 095503 and 095510 in order to check that our SAR protocol is able to accurately measure doses given in the laboratory without prior heating. First, the aliquots were optically bleached twice for 40 s (at room temperature) separated by a pause of 10,000 s, using IR diodes. They were then given a known dose of 5.5 Gy. All aliquots were then measured using the post-IR IR SAR
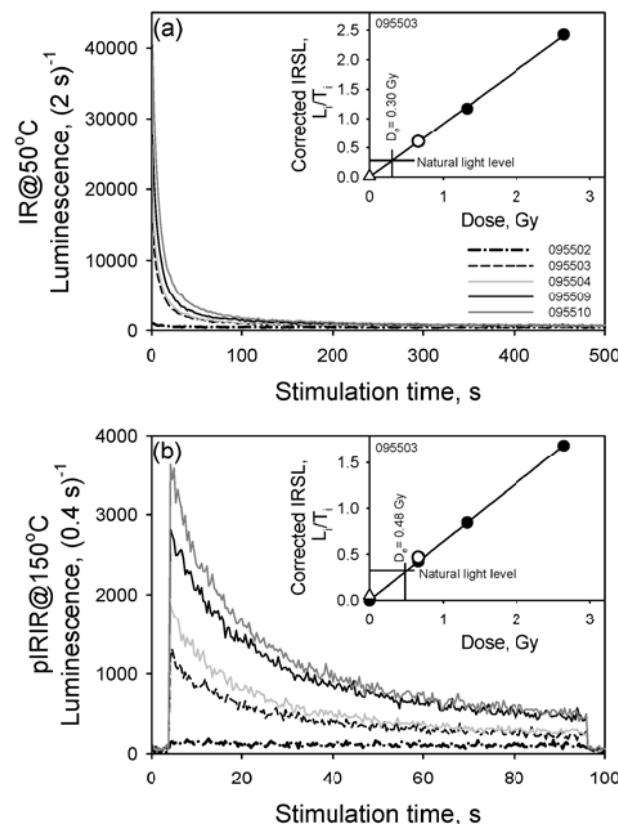

Fig. 2. *a) Stimulation decay curves of the natural IR@50°C signal, and b) stimulation decay curves of the following pIRIR@150°C signal from samples 095502, 095503, 095504, 095509 and 095510. SAR growth curves for sample 095503 are inset.*

Table 3. *Sample depth, water content, radionuclide concentrations and total dose rates.*

Sample code	Lab. code	Depth (cm)	w.c. (%)	^{226}Ra (Bq·kg⁻¹)	^{232}Th (Bq·kg⁻¹)	^{40}K (Bq·kg⁻¹)	Dose rate (Gy·ka⁻¹)
WHEL1	095509	35	276	29.1±3.9	44.7±0.4	560±60	1.80±0.08
WHEL2	095510	55	108	30.2±2.6	45.9±2.7	660±40	2.55±0.08
PAR-aeolian	095501	65	19	4.0±0.5	0.7±0.5	84±5	1.26±0.05
PAR2-0	095502	1	34	N/A	N/A	N/A	1.13±0.06
PAR2-45	095503	45	34	4.0±0.5	0.7±0.5	84±5	1.13±0.05
PAR2-75	095504	75	34	N/A	N/A	N/A	1.11±0.05

N/A –not available

protocol given in **Table 2**, but with varying preheat temperature (160–280°C in step 2) and a fixed cut-heat of 160°C (step 6). The dose recovery temperature plateaus (IR@50°C in **Fig. 4a** and pIRIR@150°C in **Fig. 4c**) suggests that the dose measurement is insensitive to preheat temperature (measured to given dose ratios are within 10% of unity); recycling ratios are close to unity at all preheat temperatures (160–280°C), and the recuperation only increases slightly with increased preheat temperature, never exceeding 0.2 Gy (**Figs. 4b** and **4d**). However, the dose could not be recovered properly in sample 095510 (the recovered dose is about 50% higher than the given dose) using the pIRIR@150°C; the reason for this is unknown.
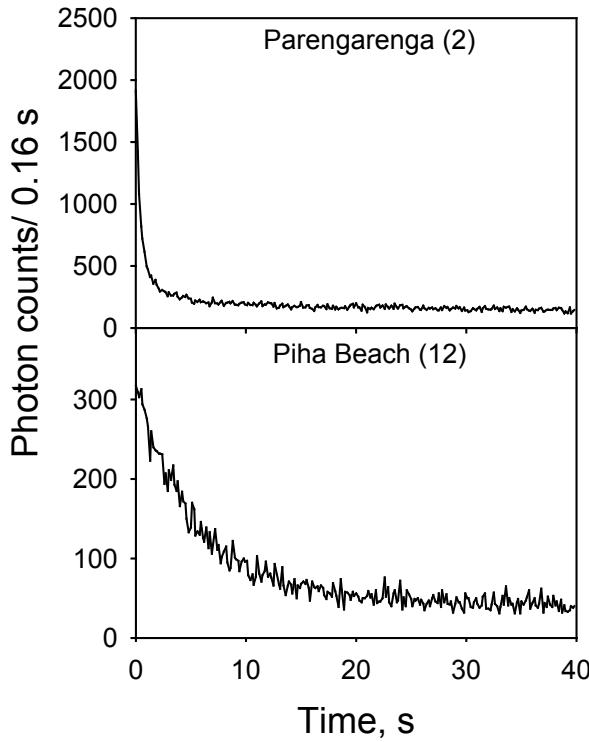
Fig. 3. *Two examples of stimulation decay curves of New Zealand quartz. The most sensitive signal (from Parengarenga) is displayed in the upper part of the diagram and the least sensitive signal (from Piha beach) is displayed in the lower part of the diagram.*

Anomalous fading test on feldspars

In the laboratory, anomalous fading was monitored by measuring the small decrease in IRSL intensity with storage time after the irradiation. For most K-feldspars the signal loss decreases linearly with the logarithm of time and this fading rate is usually quantified by the g-value (Aitken, 1985, Appendix F); this is a measure of the fading rate as a percentage of signal lost during a storage period of one decade of time (the storage period expressed in decades relative to the laboratory irradiation period). The approach by Auclair *et al.* (2003) was used to measure the anomalous fading in our samples on aliquots that were previously used for D_e determination; measurement of repeated L_i/T_i cycles were carried out with different time delays inserted after the preheating step. Time delays varied from ~0.2 h for prompt (immediate) measurements, up to ~25 h for the longest delay measurements. The g-values for both the IR@50°C and pIRIR@150°C signals were then calculated using the equation by Huntley and Lamothe (2001) and normalised to a measurement delay time (t_c) of 2 days after irradiation; this analysis assumes that the fading of the signals is logarithmic. Examples of fading rates are presented in **Fig. 5** and g-values are summarized in **Table 4**.

Fading rates for the IR@50°C signal vary between 4.1±0.5 and 9.3±0.3 %/decade, with an average of 7.1±0.3 %/decade (n=15). Despite these significant fading rates for the low temperature IR signal the pIRIR@150°C signal does not appear to show significant fading, with values ranging between -1.7±1.3 and 1.0±1.1 %/decade, with an average of 0.2±0.2 %/decade (n=15). Thus we are only justified in applying a fading correction to the IR@50°C data. It should also be noted that the range in g-values is much larger for sample 095510 than for the other samples (see **Table 4**).

5. CHRONOLOGY

Equivalent doses

Equivalent dose (D_e) measurements were undertaken on 2–24 aliquots (using both IR@50°C and pIRIR@150°C signals) resulting in dose distributions from which a mean and standard error were derived. **Fig. 6** presents four examples of such dose distributions based on the conventional IR@50°C signal and **Fig. 7** presents corresponding dose distributions based on the pIRIR@150°C signal; the obvious outliers are discarded

Table 4. *Results from the fading tests (g-values).*

Sample	095510		095501		095502		095503		095504	
	IR@50°C	pIRIR@150°C	IR@50°C	pIRIR@150°C	IR@50°C	pIRIR@150°C	IR@50°C	pIRIR@150°C	IR@50°C	pIRIR@150°C
Fading rates	9.3±0.3	-1.7±1.3	4.9±0.3	0.6±0.4	6.8±0.3	-0.2±0.8	6.2±0.4	1.0±1.4	7.2±0.4	0.3±1.0
g-value	7.6±0.7	1.0±2.3	6.3±0.5	-0.8±1.0	7.7±0.3	0.2±1.1	8.1±0.4	0.7±1.1	7.9±0.4	0.3±0.8
(%/decade)	4.1±0.5	0.5±2.4	7.9±0.3	1.0±1.1	7.3±0.3	-0.2±0.8	7.0±0.2	-0.1±0.9	7.9±0.2	0.6±0.9
Average	7.0±1.5	-0.1±0.8	6.3±0.9	0.3±0.5	7.3±0.3	-0.1±0.1	7.1±0.5	0.6±0.3	7.7±0.2	0.4±0.1

for the age calculation. It is interesting to note that the dose distributions from pIRIR@150°C measurements are wider than the dose distributions from IR@50°C measurements.

Age correction

We can now apply the age correction model of Huntley and Lamothe (2001) to the ages based on the apparently fading IR@50°C signals. The average D_e value and the average fading rate per sample were used (unfortunately there was insufficient material to determine the fading rate for sample 095509, and so the fading rate determined using the other sample (095510) from the same site was employed). These revised ages are also summarized in **Table 5** together with the fading corrected equivalent doses. On average, the IR@50°C ages become about 60% older. **Fig. 8** shows the D_e estimates based on the IR@50°C signal plotted against those from the
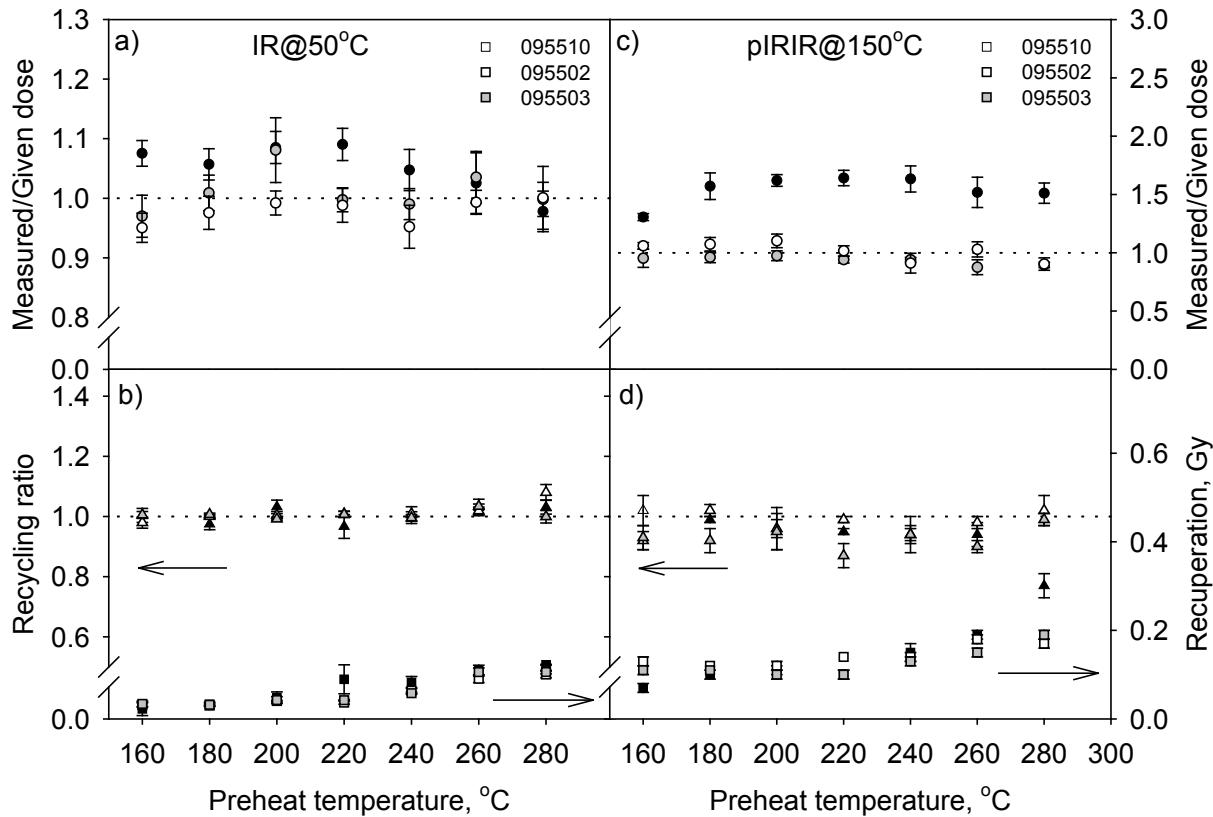
Fig. 4. *Dose recovery test, using preheat temperatures ranging between 160−280°C, for samples of sample 095510 (black), 095502 (white) and 095503 (grey). Aliquots were first optically bleached twice for 40 s (at room temperature) separated by a pause of 10 ks, using IR diodes, then given a dose of 5.5 Gy. All aliquots were then measured using the post-IR IR SAR protocol, with a fixed cut-heat of 160°C. a) Dose recovery ratio as a function of preheat temperature, when using the IR@50°C signal. b) Variation of recuperation (squares) and recycling ratio (triangles) with temperature based on the IR@50°C signal. c) Dose recovery ratio as a function of preheat temperature, when using the pIRIR@150°C signal. b) Variation of recuperation (squares) and recycling ratio (triangles) with temperature based on the pIRIR@150°C signal.*

Table 5. *Sample depth, 'n', equivalent doses based on respectively the IR@50°C signal and the pIRIR@150°C signal and the corresponding IRSL ages. Fading correction was undertaken for IRSL ages based on the IR@50°C signal.*

| Sample code	Lab. code	Depth (cm)	n	IR@50°C				pIRIR@150°C	
				D_e (Gy)	Fading corrected D_e, (Gy)	IRSL age (a)	Fading corrected IRSL age (a)	D_e (Gy)	IRSL age (a)
WHEL1	095509	35	2	1.10±0.07	2.03±0.16	610±50	1130±100	1.45±0.03	800±40
WHEL2	095510	55	23	2.41±0.07	4.44±1.09	930±40	1740±430	2.66±0.06	1050±50
PAR-aeolian	095501	65	17	0.022±0.002	0.033±0.004	18±2	27±3	0.08±0.02	60±16
PAR2-0	095502	1	23	0.033±0.002	0.054±0.004	29±2	48±4	0.05±0.01	48±6
PAR2-45	095503	45	23	0.298±0.015	0.53±0.05	265±15	470±50	0.46±0.02	400±25
PAR2-75	095504	75	15	0.300±0.004	0.56±0.02	270±15	510±30	0.40±0.01	355±20
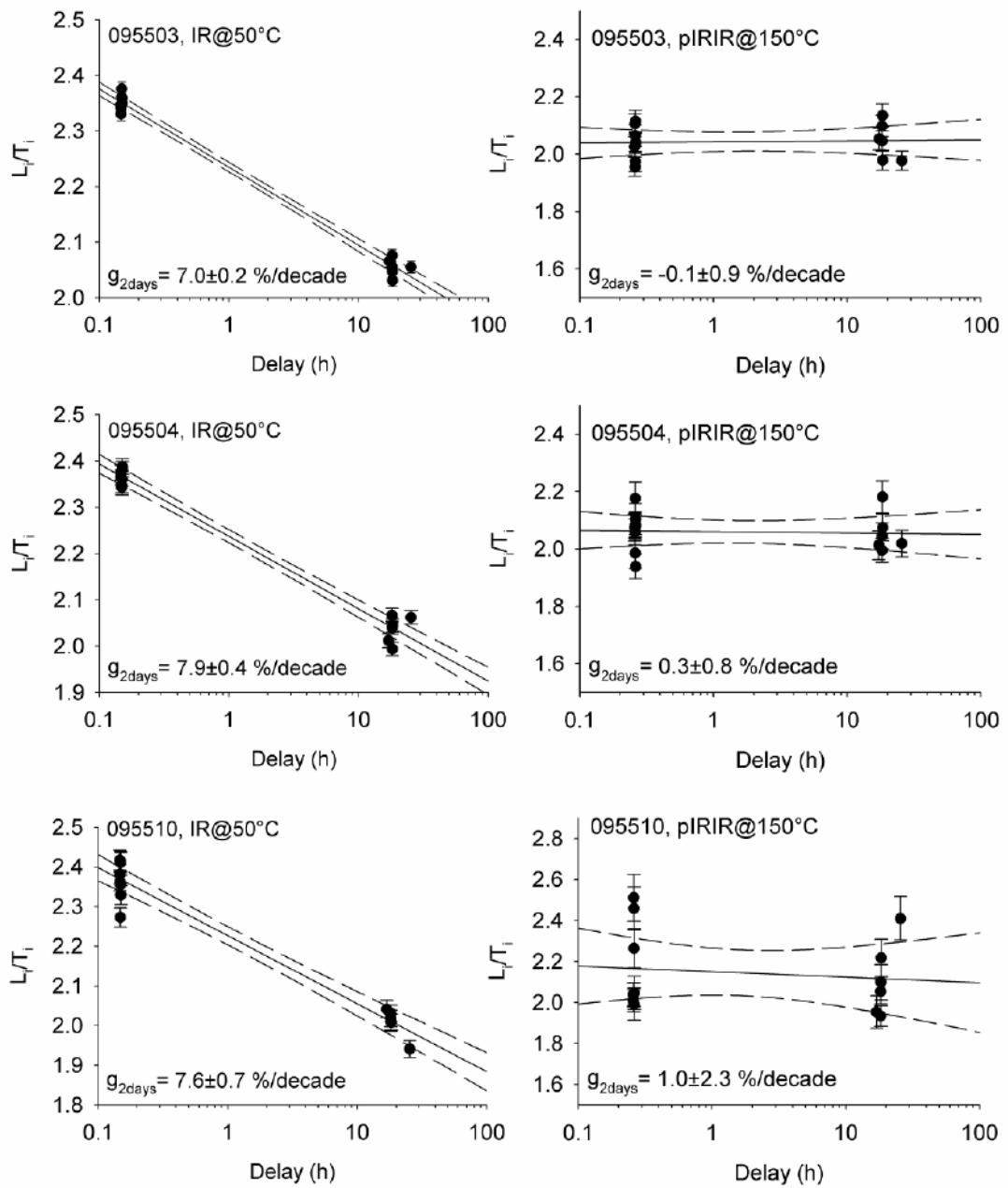
Fig. 5. *Anomalous fading plots for samples 095503, 095504, 095510. Left plots show the IR@50°C signal, right plots the pIRIR@150°C signal. The dashed lines represent a 95% confidence interval.*

pIRIR@150°C signal; open circles are without fading correction and filled circles have been corrected for fading. In general, the uncorrected IR@50°C results are closer to the pIRIR@150°C, but the deviation of the corrected and uncorrected IR@50°C from the 1:1 line is only marked for sample 095510. This is the sample giving the largest spread in g-values and the poorest dose recovery (see section 4.2). Given the good reproducibility of the uncorrected D_e values, it seems most likely that the larger g-values are in error. It is also interesting that the data (**Fig. 8**) are consistent with a line passing through the

origin, indicating that any residual dose at the time of burial (or any thermal transfer initiated during measurement) is similar for the two signals. The pIRIR@150°C results are preferred, because they do not show any fading in the laboratory, and the resulting ages range between 48±6 and 1050±50 years.

6. DISCUSSION

Although the new post-IR IR SAR protocol has performed satisfactorily in a dose recovery test (except for
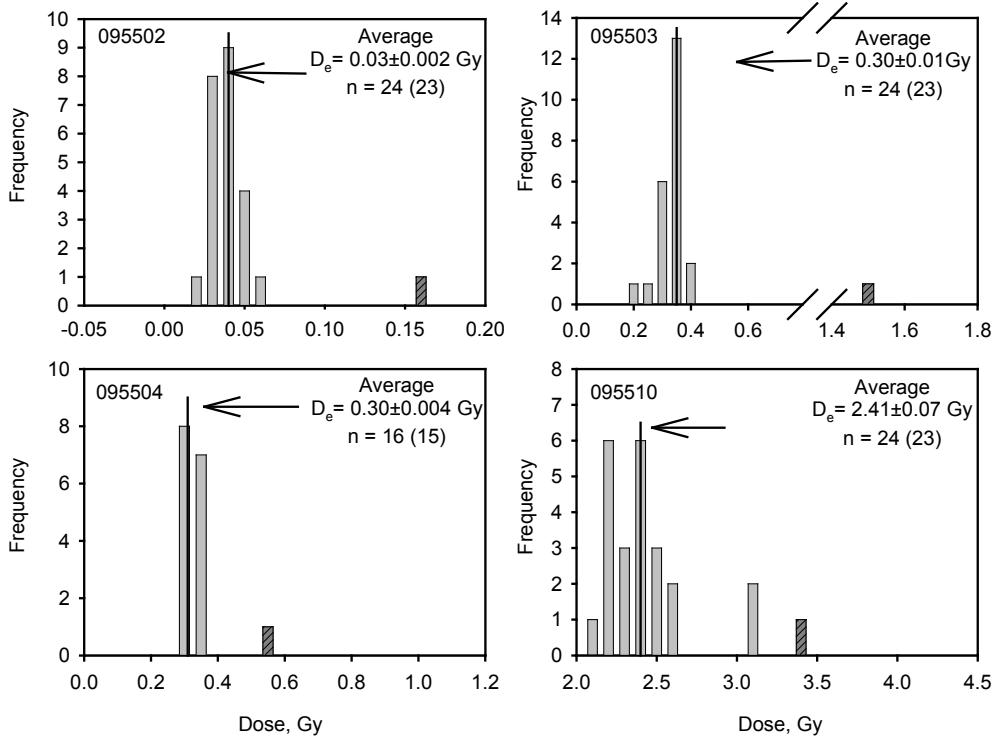
Fig. 6. *Dose distributions of samples 095502, 095503, 095504 and 095510. The IR@50°C signal is used for these plots. 'n' is the number of observations. The number in brackets is the number of aliquots included in the calculation of the mean; obvious outliers are displayed as dark grey dashed bars.*
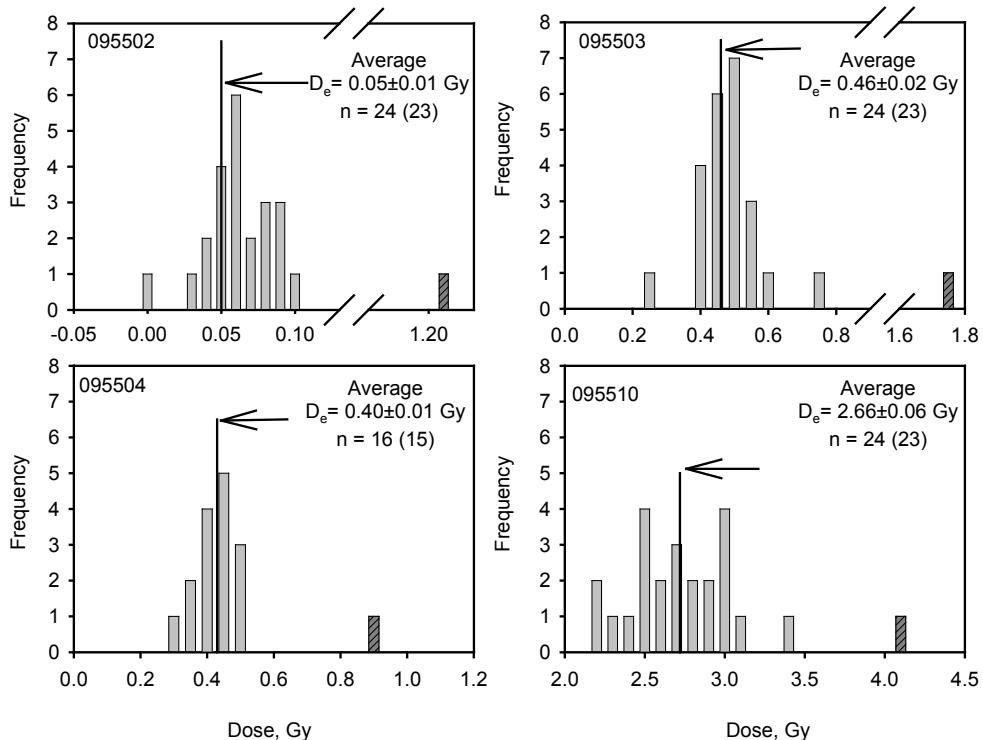

Fig. 7. *Dose distributions of sample 095502, 095503, 095504 and 095510. The pIRIR@150°C signal is used for these plots. 'n' is the number of observations. The number in brackets is the number of aliquots included in the calculation of the mean; obvious outliers are displayed as dark grey dashed bars.*
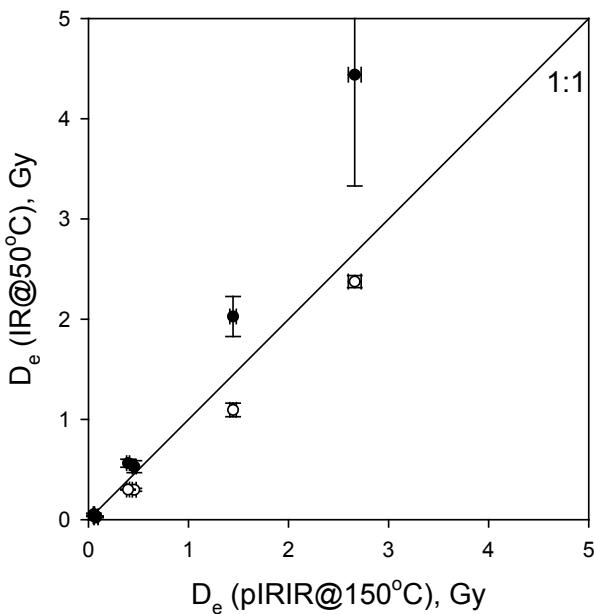
Fig. 8. *Equivalent dose estimates based on the IR@50°C signal plotted against the equivalent dose estimates based on the pIRIR@150°C signal; open circles are without fading correction and filled circles are fading corrected.*

sample 095510) this is not a complete test of the reliability of the SAR protocol because in nature the environmental dose rate is about 10^9 less than in the laboratory. The most comprehensive test is to date known-age samples. Unfortunately, independent age information is scarce in this study. The result from the aeolian sample (095501) from Parengarenga is our best attempt to date a known-age deposit. The coastal dune from which the material was sampled is known to have formed since 1982 based on sequential levelling surveys (Parnell *et al.* 2003; pers. comm.) and the age is estimated to lie between modern and 27 years old, compared to an IRSL age of 60±16 years.

It is known that quartz in such shallow coastal environments is very likely to be well-bleached (Madsen and Murray, 2009) but the solar resetting process is slower for feldspar than for quartz (e.g. Godfrey-Smith *et al.*, 1988). Thus we cannot be certain that these feldspar samples have been fully reset, and that residual doses at burial can be neglected. One way of evaluating minimum residual doses is to consider the modern surface sample (095502) and the very recent aeolian material (095501; discussed above) from Parengarenga. The total dose (IR@50°C and pIRIR@150°C) in the modern surface (095502) from Parengarenga was in the range 30–50 mGy (**Table 5**). This sample included the top 5 cm of the inter-tidal sediment core; if the sedimentation rate is assumed to be about 2 mm·a^{-1}, then this means that the average age of the 5 cm slice is 12.5 years, corresponding to a dose of ~14 mGy. This suggests that residual doses are ~20 mGy for IR@50°C signals and ~35 mGy for pIRIR@150°C

signals. The very recent aeolian material (095501) is known to have a finite age of 0–27 years (see above). Using the mid-point of this range as our age estimate gives an expected dose of ~20 mGy. The observed total doses were 22 mGy based on IR@50°C signals (implying a residual of only ~3 mGy) and 80 mGy based on pIRIR@150°C signals (residual of ~60 mGy). It is reasonable to assume that the aeolian sand will have received much more light exposure than the upper layers of marine sediment. This suggests that in both cases the signals are reset as completely as possible, but that there is some irreducible minimum dose that cannot be readily bleached, ~10 mGy for the IR@50°C signals and ~50 mGy for pIRIR@150°C. It seems likely that these values reflect thermal transfer from light insensitive traps, rather than actual incomplete bleaching of light sensitive traps.

This research was undertaken to determine whether it is possible to reconstruct the response to a stable or falling sea-level at coastal sites in New Zealand. As a result, this study was directed primarily towards investigating the suitability of these New Zealand deposits for dating very recent deposition events. Because of this, there is only a limited number of luminescence ages, but nevertheless some preliminary interpretation can be made. About half a metre of material has accumulated on the salt-marsh in Whanganui Inlet during the last millennium; a preliminary sedimentation rate for this salt-marsh is in the range 0.5–0.8 mm·a^{-1} (when averaging between 0–55 cm or 35–55 cm depth). Thus accumulation has continued in supra-tidal areas in Whanganui Inlet during the last ~1000 years, despite the slowly decreasing relative sea-level resulting from a local tectonic uplift rate of 0–1 mm·a^{-1} (Litchfield, pers. comm. 2010). The core retrieved from Parengarenga Harbour gives a preliminary sedimentation rate of ~2 mm·a^{-1} (when averaging between 0–75 cm). This estimate seems relatively high, given that sea-level in this area has been almost stable since the mid-Holocene (~6500 years ago; Gibb, 1986). However, sampling was undertaken in near proximity to one of the large tidal channels, and so this sedimentation rate may relate more to channel migration rather than simple tidal flat deposition. In the lateral displacement of tidal channels large amounts of sediment are able to accumulate almost instantaneously as point-bar sedimentation, giving rise to a sediment packet with apparent constant ages with depth (Fruergaard *et al.* 2011). This is presumably the reason why almost identical ages are observed at 45 cm and 75 cm depth in the Parengarenga core.

7. CONCLUSIONS

This study has tested a new protocol for K-feldspar luminescence dating on young coastal sediments from New Zealand, and IRSL ages ranging between 48–1050 years have been obtained. One of the major challenges associated with IRSL dating of K-feldspar is the signal

loss due to anomalous fading, which necessitates the use of age correction models. Our new protocol appears to sample a new and apparently more stable luminescence signal by measuring IRSL at elevated temperature (150°C) immediately after a long IR@50°C stimulation (the pIRIR@150°C signal). We are unable to detect significant laboratory fading of this pIRIR@150°C signal (g-values range between -1.7±1.3 and 1.0±1.1 %/decade) whereas the conventional IR@50°C signal gives fading rates of ~7 %/decade. The youngest ages observed here (48±6 years for inter-tidal sediment and 60±16 years for aeolian sediment) were only slightly older than the likely depositional ages of these deposits, indicating considerable potential for the dating of recent coastal deposits in New Zealand.

ACKNOWLEDGEMENTS

REFERENCES

Aitken MJ, 1985. *Thermoluminescence dating*. London, Academic Press Inc: 359pp

Almond PC, Moar NT and Lian OB, 2001. Reinterpretation of the glacial chronology of South Westland, New Zealand. *New Zealand Journal of Geology and Geophysics* 44(1): 1-15, DOI 10.1080/00288306.2001.9514917.

Almond PC, Shanhun FL, Rieser U and Shulmeister J, 2007. An OSL radiocarbon and tehpra isochron-based chronology for Birdlings flat loess at Ahuriri Quarry, Banks Peninsula, Canterbury, New Zealand. *Quaternary Geochronology* 2(1-4): 4-8, DOI 10.1016/j.quageo.2006.06.002.

Armour RK and Kennedy DM, 2005. Comparative palynomorph signals of vegetation change preserved in an adjacent peat swamp and estuary in North-West Nelson, New Zealand. *New Zealand Journal of Botany* 43(2): 451-465, DOI 10.1080/0028825X.2005.9512967.

Auclair M, Lamothe M and Huot S, 2003. Measurement of anomalous fading for feldspar IRSL using SAR. *Radiation Measurements* 37(4-5): 487-492, DOI 10.1016/S1350-4487(03)00018-0.

Auclair M, Lamothe M, Lagroix F and Banerjee SK, 2007. Luminescence investigations of loess and tephra from Halfway House section, Central Alaska. *Quaternary Geochronology* 2(1-4): 34-38, DOI 10.1016/j.quageo.2006.05.009.

Berger GW, Almond PC and Pillans BJ, 2001. Luminescence dating and glacial stratigraphy in Westland, New Zealand. *New Zealand Journal of Geology and Geophysics* 44(1): 25-35, DOI 10.1080/00288306.2001.9514919.

Bøtter-Jensen L, Andersen CE, Duller GAT and Murray AS, 2003. Developments in radiation, stimulation and observation facilities in luminescence measurements. *Radiation Measurements* 37(4-5): 535-541, DOI 10.1016/S1350-4487(03)00020-9.

Buylaert JP, Murray AS, Thomsen KJ and Jain M, 2009. Testing the potential of an elevated temperature IRSL signal from K-feldspar. *Radiation Measurements* 44(5-6): 560-565, DOI 10.1016/j.radmeas.2009.02.007.

Buylaert JP, Huot S, Murray AS and Van den Haute P, 2011. Infrared stimulated luminescence dating of an Eemian (MIS 5e) site in Denmark using K-feldspar. *Boreas* 40(1): 46-56, DOI 10.1111/j.1502-3885.2010.00156.x.

Cooper AF and Kostro F, 2006. A tectonically uplifted marine shoreline deposit, Knights Point, Westland, New Zealand. *New Zealand Journal of Geology and Geophysics* 49(2): 203-216, DOI 10.1080/00288306.2006.9515160.

Davids F, Duller GAT and Roberts HM, 2010. Testing the use of feldspars for optical dating of hurricane overwash deposits. *Quaternary Geochronology* 5(2-3): 125-130, DOI 10.1016/j.quageo.2009.03.001.

Davidson RJ, 1990. *A report on the ecology of Whanganui Inlet, northwest Nelson*. Occasional Publication, vol. 2. Department of Conservation, Nelson/Marlborough Conservancy, New Zealand.

Duller GAT, 1994a. Luminescence dating of sediments using single aliquots: New procedures. *Quaternary Science Reviews* 13(2): 149-156, DOI 10.1016/0277-3791(94)90041-8.

Duller GAT, 1994b. Luminescence dating using feldspars: a test case from southern North Island, New Zealand. *Quaternary Science Reviews* 13(5-7): 423-427, DOI 10.1016/0277-3791(94)90053-1.

Duller GAT, 1996. The age of the Koputaroa dunes, southwest North Island, New Zealand. *Palaeogeography, Palaeoclimatology, Palaeoecology* 121(1-2): 105-114, DOI 10.1016/0031-0182(96)00053-3.

Fruergaard M, Andersen TJ, Madsen AT, Christensen L, Nielsen LH, Johannessen PN, Murray AS and Pejrup M, 2011. Punctuated sedimentation resulting from channel migration in a shallow sand-dominated micro-tidal lagoon, Northern Wadden Sea, Denmark. *Marine Geology* 280(1-4): 91-104, DOI 10.1016/j.margeo.2010.12.003.

Gibb JG, 1986. A New Zealand regional Holocene eustatic sea-level curve and its application to determination of vertical tectonic movements. *Royal Society New Zealand Bulletin* 14: 377-395.

Godfrey-Smith DL, Huntley DJ and Chen WH, 1988. Optically dating studies of quartz and feldspar sediment extracts. *Quaternary Science Reviews* 7(3-4): 373-380, DOI 10.1016/0277-3791(88)90032-7.

Hayes MO, 1979. Barrier island morphology as a function of tidal influence and wave regime. In: Leathermann SP, ed., *Barrier Islands*. Academic Press, New York: 1-27.

Heath RA, 1975. Stability of some New Zealand coastal inlets. *New Zealand Journal of Marine and Freshwater Research* 9(4): 449-457, DOI 10.1080/00288330.1975.9515580.

Heath RA, 1976. Broad classification of New Zealand inlets with emphasis on residence times. *New Zealand Journal of Marine and Freshwater Research* 10(3): 429-444, DOI 10.1080/00288330.1976.9515628.

Huntley DJ and Baril MR, 1997. The K content of the K-feldspars being measured in optical dating or in thermoluminescence dating. *Ancient TL* 15: 11-13.

Huntley DJ and Hancock RGV, 2001. The Rb contents of the K-feldspar grains being measured in optical dating. *Ancient TL* 19: 43-46.

Huntley DJ and Lamothe M, 2001. Ubiquity of anomalous fading in K-feldspars and the measurement and correction for it in optical dating. *Canadian Journal of Earth Science* 38(7): 1093-1106, DOI 10.1139/e01-013.

Jacobs Z, 2008. Luminescence chronologies for coastal and marine sediments. *Boreas* 37(4): 508-535, DOI 10.1111/j.1502-3885.2008.00054.x.

Kennedy DM, Tannock KL, Crozier MJ and Rieser U, 2007. Boulders of MIS 5 age deposited by a tsunami on the coast of Otago, New Zealand. *Sedimentary Geology* 200(3-4): 222-231, DOI 10.1016/j.sedgeo.2007.01.005.

Kennedy DM, Paulik R and Millar M, 2008. Infill of a structurally controlled estuary: An example from southern Whanganui Inlet, New Zealand. *New Zealand Geographer* 64(1): 20-33, DOI 10.1111/j.1745-7939.2008.00124.x.

Litchfield NJ and Lian OB, 2004. Luminescence age estimates of Pleistocene marine terrace and alluvial fan sediments associated with tectonic activity along coastal Otago, New Zealand. *New Zealand Journal of Geology and Geophysics* 47(1): 29-37, DOI 10.1080/00288306.2004.9515035.

Litchfield N, pers. comm. 2010. GNS Science, Lower Hutt, Wellington, New Zealand.

Madsen AT, Murray AS, Andersen TJ, Pejrup M and Breuning-Madsen H, 2005. Optically stimulated luminescence dating of young estuarine sediments: a comparison with ^{210}Pb and ^{137}Cs dating. *Marine Geology* 214(1-3): 251-268, DOI 10.1016/j.margeo.2004.10.034.

Madsen AT and Murray AS, 2009. Optically stimulated luminescence dating of young sediments: a review. *Geomorphology* 109(1-2): 3-16, DOI 10.1016/j.geomorph.2008.08.020.

Murray AS, Marten R, Johnston A and Martin P, 1987. Analysis for naturally occuring radionuclides at environmental concentrations by gammaspectrometry. *Journal of Radioanalytical and Nuclear Chemistry* 115(2): 263-288, DOI 10.1007/BF02037443.

Murray AS and Wintle AG, 2000. Luminescence dating of quartz using an improved single-aliquot Regenerative-dose protocol. *Radiation Measurements* 32(1): 57-73, DOI 10.1016/S1350-4487(99)00253-X.

Murray AS and Wintle AG, 2003. The single aliquot regenerative dose protocol: potential for improvements in reliability. *Radiation Measurements* 37(4-5): 377-381, DOI 10.1016/S1350-4487(03)00053-2.

Nichol SL, 2002. Morphology, stratigraphy and origin of last interglacial beach ridges at Bream Bay, New Zealand. *Journal of Coastal Research* 18: 149-159.

Nichol SL, Lian OB and Carter CH, 2003. Sheet-gravel evidence for a late Holocene tsunami run-up on beach dunes, Great Barrier Island, New Zealand. *Sedimentary Geology* 155(1-2): 129-145, DOI 10.1016/S0037-0738(02)00191-4.

Olley J, Murray AS and Roberts RG, 1996. The effects of disequilibria in the uranium and thorium decay chains on burial dose rates in fluvial sediments. *Quaternary Science Reviews* 15(7): 751-760, DOI 10.1016/0277-3791(96)00026-1.

Parnell KE, Hosking PL and Nichol SL, 2003 (pers. comm.). *Parengarenga Monitoring Programme. Summary of surveys August 1998 – February 2003 and Summary of all surveys 1982–2003.* Unpublished Report prepared for ACI New Zealand Glass Manufacturers Ltd.

Pillans B, Kohn BP, Berger G, Froggatt P, Duller G, Alloway B and Hesse P, 1996. Multi-method dating comparison for mid-Pleistocene Rangitawa tephra, New Zealand. *Quaternary Science Reviews* 15(7): 641-653, DOI 10.1016/0277-3791(96)00035-2.

Prescott JR and Hutton JT, 1994. Cosmic ray contributions to dose rates for luminescence and ESR dating: large depths and long-term variations. *Radiation Measurements* 23(2-3): 497-500, DOI 10.1016/1350-4487(94)90086-8.

Preusser F, Ramseyer K and Schlüchter C, 2006. Characterisation of low OSL intensity quartz from the New Zealand Alps. *Radiation Measurements* 41(7-8): 871-877, DOI 10.1016/j.radmeas.2006.04.019.

Pritchard J, Osbourne P, Parnell K and Nichol SL, 1998. Sediment transport trends, Parengarenga Harbour. In: Forer PC, Lumsden J and Perry PJ, eds. *Proceedings of the 18th New Zealand Geographical Society Conference*, vol. 18. Dunidin, New Zealand.

Schofield JC, 1970. Coastal sands of Northland and Auckland. *New Zealand Journal of Geology and Geophysics* 13: 767-823.

Rees-Jones J, Rink WJ, Norris RJ and Litchfield NJ, 2000. Optical luminescence dating of uplifted marine terraces along the Akatore Fault near Dunedin, South Island, New Zealand. *New Zealand Journal of Geology and Geophysics* 43(3): 419-424, DOI 10.1080/00288306.2000.9514898.

Shulmeister J and Kirk RM, 1996. Holocene history and a thermoluminescence based chronology of coastal dune ridges near Leithfield, North Canterbury, New Zealand. *New Zealand Journal of Geology and Geophysics* 39(1): 25-32, DOI 10.1080/00288306.1996.9514692.

Shulmeister J, Soons JM, Berger GW, Harper M, Holt S, Moar N and Carter JA, 1999. Environmental and sea-level changes on Banks Peninsula (Canterbury, New Zealand) through three glaciation – interglaciation cycles. *Palaeogeography, Palaeoclimatology, Palaeoecology* 152(1-2): 101-127, DOI 10.1016/S0031-0182(99)00035-8.

Thomsen KJ, Murray AS, Jain M and Bøtter-Jensen L, 2008. Laboratory fading rates of various luminescence signals from feldspar-rich sediment extracts. *Radiation Measurements* 43(9-10): 1474-1486, DOI 10.1016/j.radmeas.2008.06.002.

Wallinga J, Bos AJJ, Dorenbos P, Murray AS and Schokker J, 2007. A test case for anomalous fading correction in IRSL dating. *Quaternary Geochronology* 2(1-4): 216-221, DOI 10.1016/j.quageo.2006.05.014.

Wellman HW, 1962. Holocene of the North Island of New Zealand: a coastal reconnaissance. *Transactions of the Royal Society of New Zealand Geology* 1(5): 29-99.

Wintle AG, 1973. Anomalous fading of thermoluminescence in mineral samples. *Nature* 245(5421): 143-144, DOI 10.1038/245143a0.